Footprint and Physical Size of Low-frequency Earthquakes – Evidence From Real and Synthetic Seismograms

Chao Song[1] and Allan Rubin[1]

[1]Affiliation not available

March 15, 2024

Footprint and Physical Size of Low-frequency Earthquakes – Evidence From Real and Synthetic Seismograms

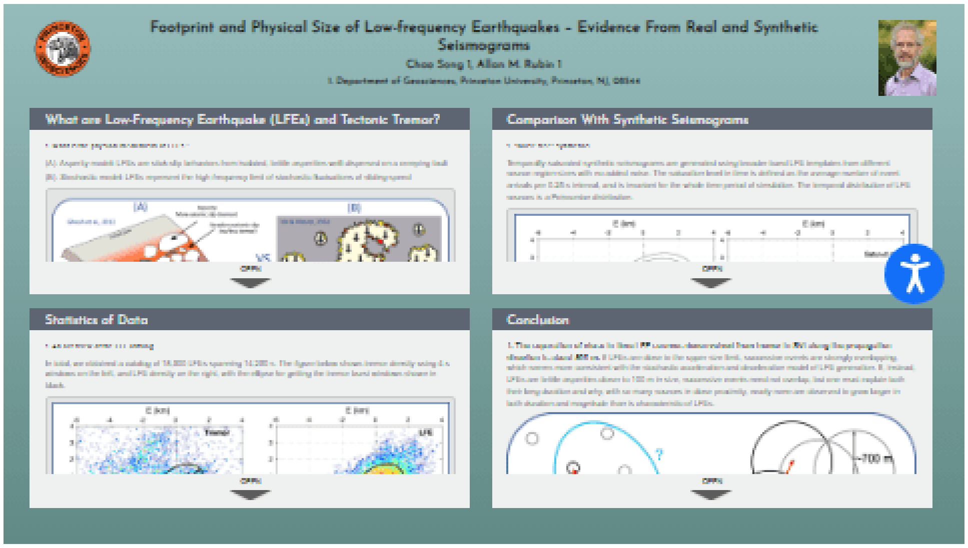

Chao Song 1, Allan M. Rubin 1

1. Department of Geosciences, Princeton University, Princeton, NJ, 08544

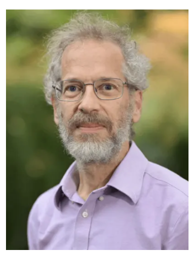

PRESENTED AT:

AGU23 WIDE. OPEN. SCIENCE.

WHAT ARE LOW-FREQUENCY EARTHQUAKE (LFES) AND TECTONIC TREMOR?

1. What is the physical mechanism of LFEs?

(A). Asperity model: LFEs are stick-slip behaviors from isolated, brittle asperities well-dispersed on a creeping fault

(B). Stochastic model: LFEs represent the high-frequency limit of stochastic fluctuations of sliding speed

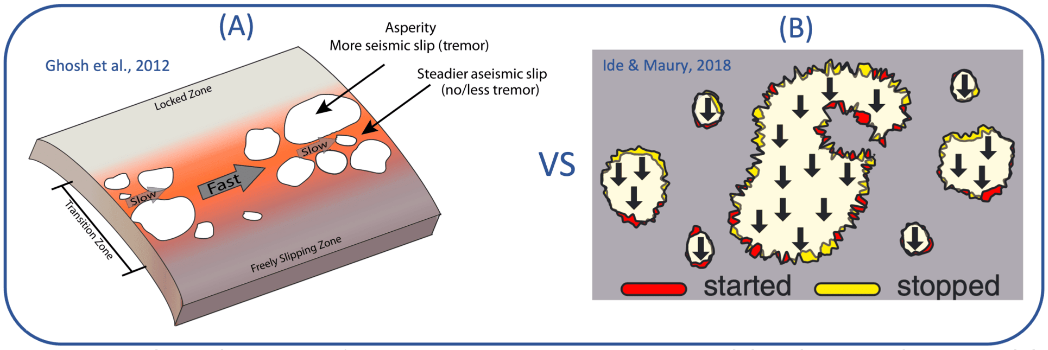

Fig. 1 Two end-member views of LFEs (or tremor). (A) Asperity model and (B) Stochastic model

In view (A), an LFE source has frictional properties different from its surroundings, and each represents a co-located acceleration/deceleration (*1*).

In view (B), the stochastic, extended-source-region model of Ide (*2*), the accelerations and decelerations that comprise "LFEs" are not necessarily co-located, and most of the underlying seismic moment lies outside the roughly 1-8 Hz band of good signal-to-noise ratio.

2. One of the unknowns --- phyiscal dimension of LFEs

Estimates of the size range from 100 m (if they have a stress drop similar to regular earthquakes) to 700 m (if they are elastodynamic events given a ~0.25-s duration and a reduced shear wave speed).

Can high-resolution LFE locations place constraints on their physical dimension, which would then give some hint on the physical mechanism of tectonic tremor? The answer is likely yes!

Below is an example of tremor seismograms carrying a high coherence between stations for dozens of seconds, which implies a train of LFE-template-like signals coming from a compact area. This encourages us to obtain an LFE catalog with a temporal resolution conceivably as high as one event per LFE duration (resolve every coherent wiggle!).

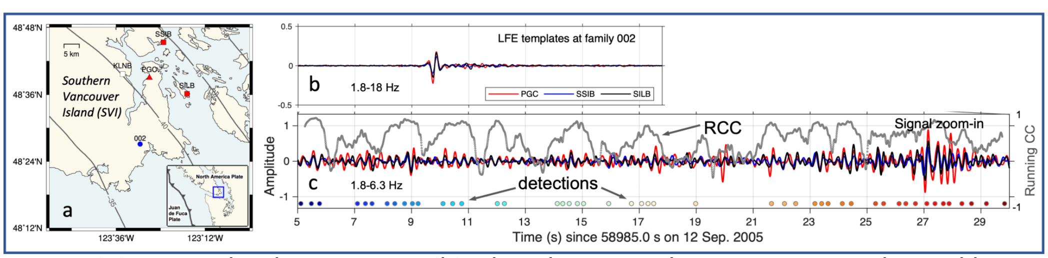

Fig. 2 (a) Station distribution at SVI. (b) Filtered LFE templates at 3 stations obtained by a stacking of thousands of LFEs. (c) Filtered tremor seismograms at the same 3 stations for a 25-s window annotated with running cross-correlation (RCC; a proxy for coherence) and LFE detections.

3. Iterative deconvolution of tremor

We obtain the LFE catalog from an iterative time-domain deconvolution (*3-5*) of tremor records, using stacked LFE templates as the empirical Green's functions.

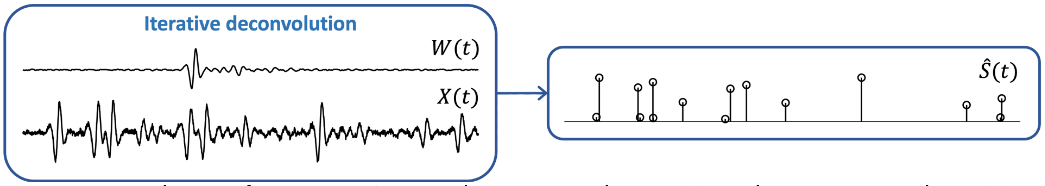

Fig. 3 Deconvolution of tremor X(t) using the LFE template W(t) to obtain LFE impulses S(t) at a single station. We do this at 3 stations independently, and then group the impulses to detect and locate the LFEs.

STATISTICS OF DATA

1. An overview of the LFE catalog

In total, we obtained a catalog of 18,500 LFEs spanning 14,250 s. The figure below shows tremor density using 4-s windows on the left, and LFE density on the right, with the ellipse for getting the tremor burst windows shown in black.

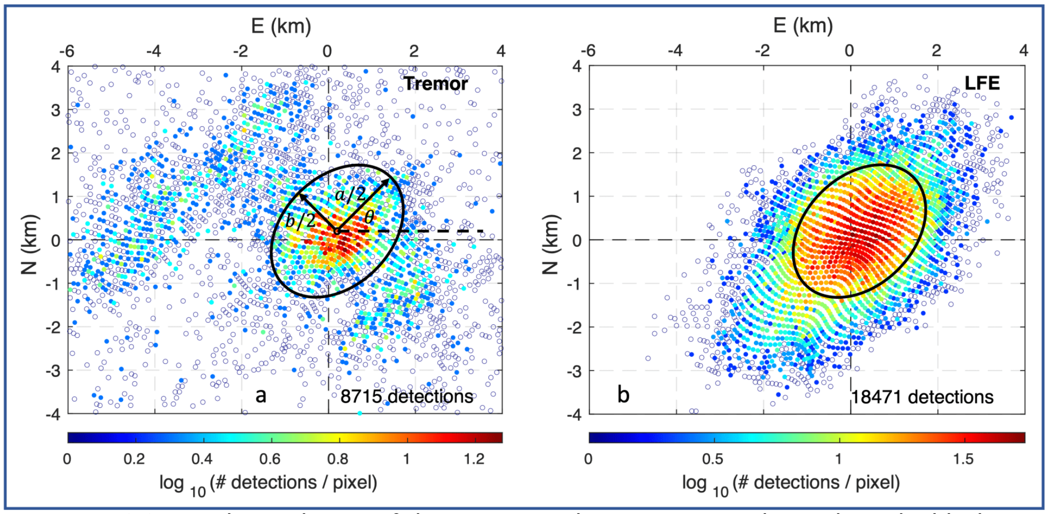

Fig. 4 (a) Cumulative density of the tremor catalog using 4-s windows, where the black ellipse roughly contour the region with the highest activity. (b) Cumulative density of the deconvolved LFE catalog from tremor within the ellipse

2. Spatial separation of LFE sources

Our 3-station deconvolution catalog shows that the close-in-time sources are separated by about 500 m along the propagation direction. This suggests that if LFEs are close to the upper size limit, successive events are strongly overlapping, which seems more consistent with the stochastic acceleration and deceleration model of LFE generation. If, instead, LFEs are brittle asperities closer to 100 m in size, successive events need not overlap, but one must explain both their long duration and why, with so many sources in close proximity, nearly none are observed to grow larger in both duration and magnitude than is characteristic of LFEs.

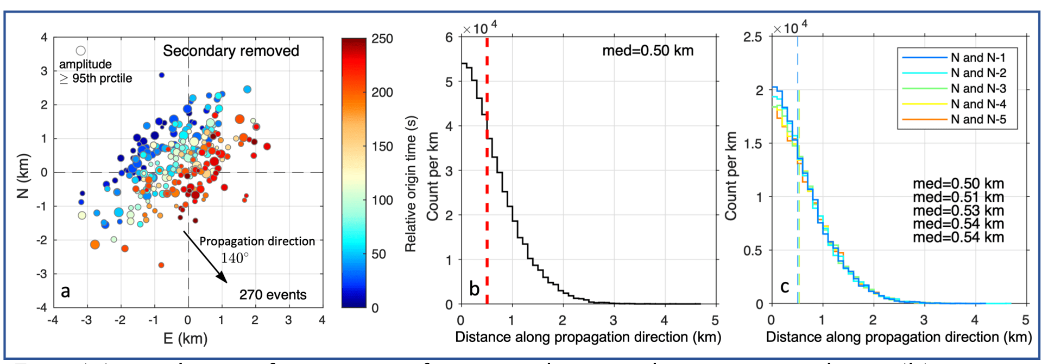

Fig. 5 (a) Distribution of LFE sources for a 250-s burst window in space and time. (b) Distance along the propagation direction from each source to all others that arrive within 2 s. (c) Similar as (b), but for source pairs N & N-m, up to m=5.

3. Saturation of tremor seismograms in time with LFE sources

Over an amplitude range that spans an order of magnitude, tremor seismograms from SVI appear saturated with LFE arrivals, in the sense that inter-event times are less than the characteristic LFE duration (~0.25 s). Quantitatively, about 46% of consecutive LFEs detected via iterative deconvolution are separated by roughly this duration.

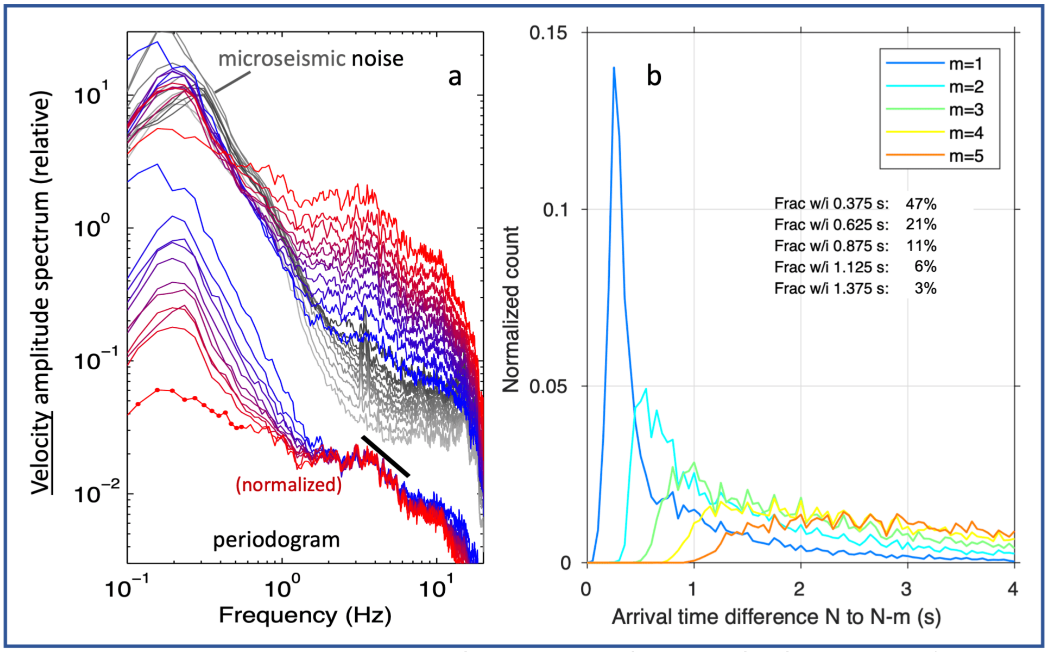

Fig. 6 Tremor seismograms are saturated in time. (a) Velocity amplitude spectrum of tremor seismograms, spanning over an order of magnitude. (b) Arrival time difference of deconvolved sources N to N-m.

The saturation seems independent of tremor amplitude, meaning that quiet tremor is not obviously less saturated in time than loud tremor, consistent with Ide's stochastic model.

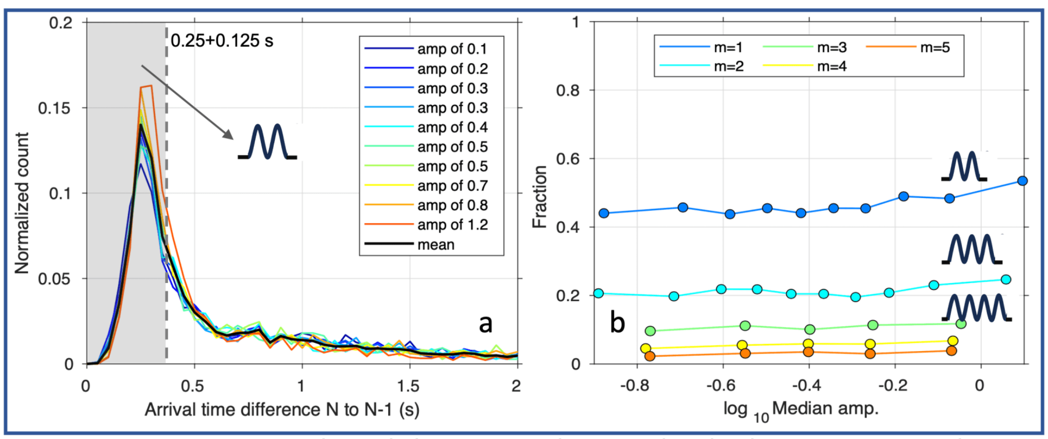

Fig. 7 Quiet tremor is not obviously less saturated in time than loud tremor. (a): Arrival time difference of deconvolved sources N to N-1, binned by source amplitude. (b): Fraction of arrival time difference N to N-m that is within m*0.25+0.125 s.

COMPARISON WITH SYNTHETIC SEISMOGRAMS

1. "Noise-free" synthetics

Temporally-saturated synthetic seismograms are generated using broader-band LFE templates from different source-region sizes with no added noise. The saturation level in time is defined as the average number of event arrivals per 0.25-s interval, and is invariant for the whole time period of simulation. The temporal distribution of LFE sources is a Poissonian distribution.

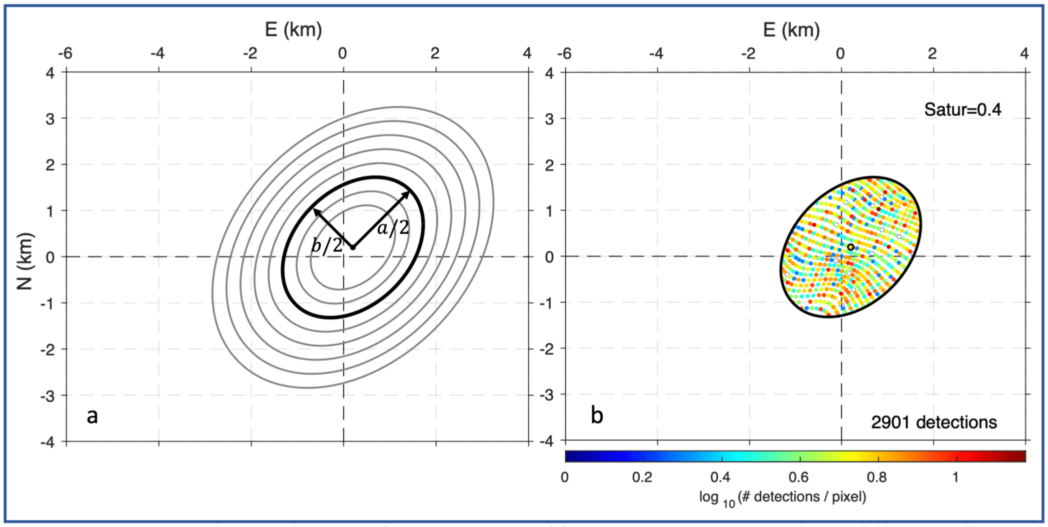

Fig. 8 Generation of noise-free synthetics. (a) LFE-like sources may come from different elliptical region sizes. (b) Within each region, saturated sources are randomly distributed and their origin times are Poissonian processes.

The cross-correlation (CC) between synthetic seismograms for the whole-window at 3 stations are obtained, as well as a deconvolution of synthetics in the same way as that of data. The arrival time difference N to N-1 of deconvolved sources are also analyzed. These statistics are compared with those of data as below.

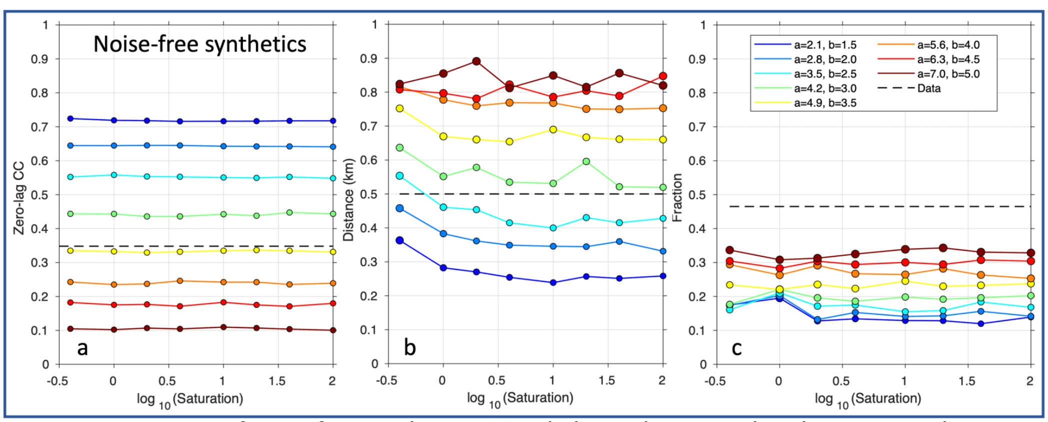

Fig. 9 Statistics of noise-free synthetics. (a) Whole-window CC values between synthetic seismograms at station pairs. (b) Distance along the min-error direction from each LFE source to all others that arrive within 2 s. Min-error direction here is essentially the same as the propagation direction of data. Sources are deconvolved from synthetics. (c) Fraction of arrival time difference N to N-1 that is within 0.25*1+0.125 s.

When there is no noise, CC values are almost independent of the saturation of synthetics. To match the observed CC value, the source area may not be exceed 4.9 km x 3.5 km. To match the observed median distance between nearly-consecutive sources, the source area may not be exceed 4.2 km x 3 km. However, all simulations fail to reproduce the arrival time difference N to N-1, and could not reach the high fraction of arrival time difference that is within 0.25*1+0.125 s. This may indicate that real data is much more clustered in time.

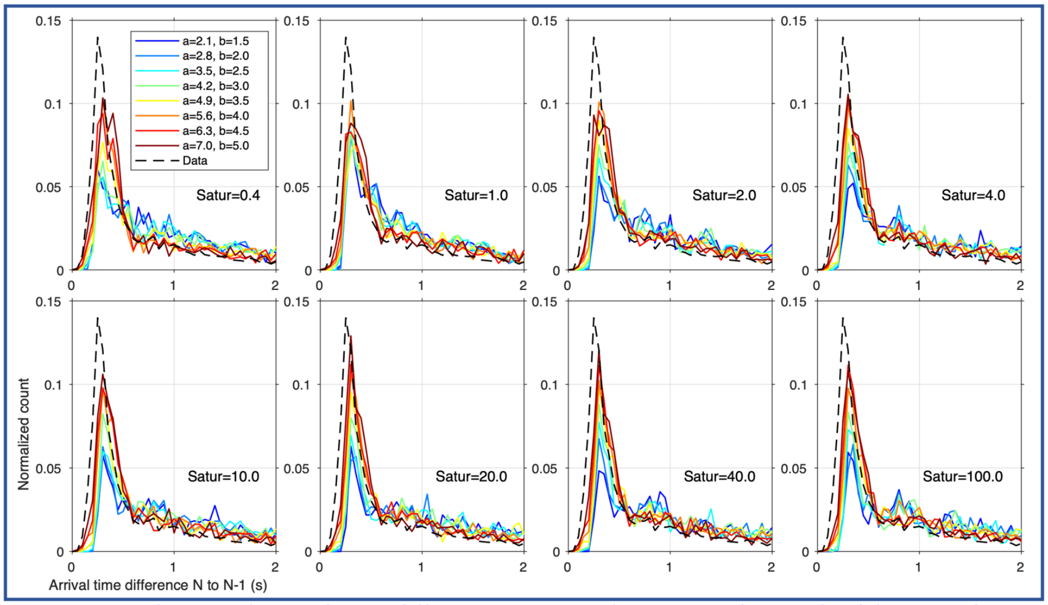

Fig. 10 Distribution of arrival time difference N to N-1 for sources deconvolved from synthetic seismograms with various saturation from different region sizes.

2. "Single-spot" synthetics

Temporally-saturated synthetic seismograms are generated using LFE templates from a single spot with different noise levels. For a certain saturation, noise of a level of 1 (or 100%) is assembled by the amplitude spectrum of single-spot synthetics of that saturation, and a randomized phase spectrum.

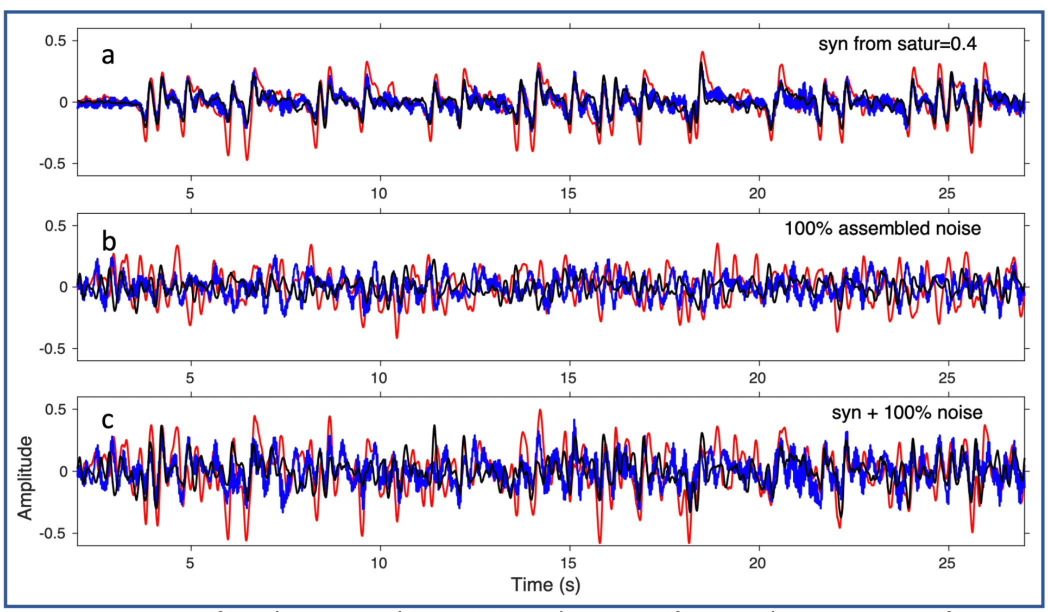

Fig. 11 Generation of single-spot synthetics. (a) Synthetic waveforms with a saturation of 0.4 at 3 stations from a single spot. (b) 100% noise assembled from (a). (c) New synthetics by adding (b) to (a).

Similar to "noise-free" synthetics, CC and deconvolution are implemented to the "single-spot" synthetics. A similar comparison of statistics with data is shown as below.

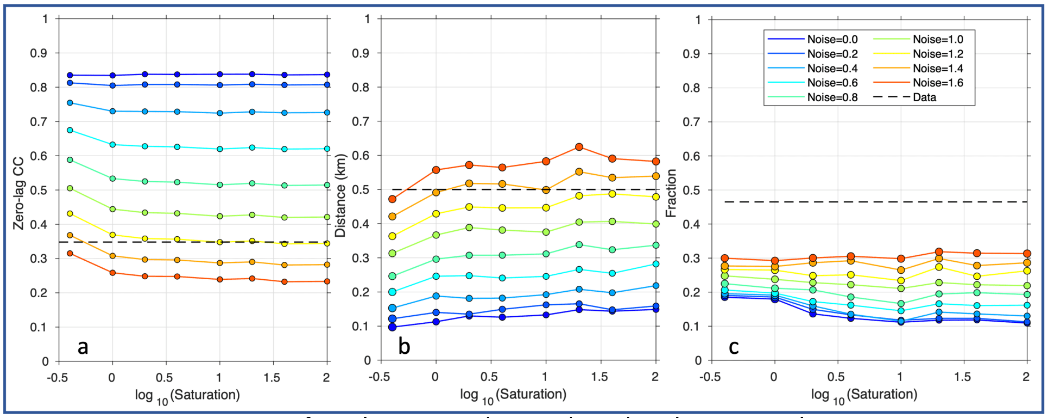

Fig. 12 Statistics of single-spot synthetics plotted in the way similar to Fig. 9.

CC values are slightly more sensitive to saturation than in the case of "noise-free" synthetics. To match both the observed CC value and median distance between nearly-consecutive sources, the noise level probably would be around 120-140%. This end-member simulation also could not reproduce the high-clustering in time of neighboring events from observation, implying that the high-clustering nature of data is unlikely to be due to the presence of noise. In the future work, we might carry simulations from combining some noise level with different region sizes.

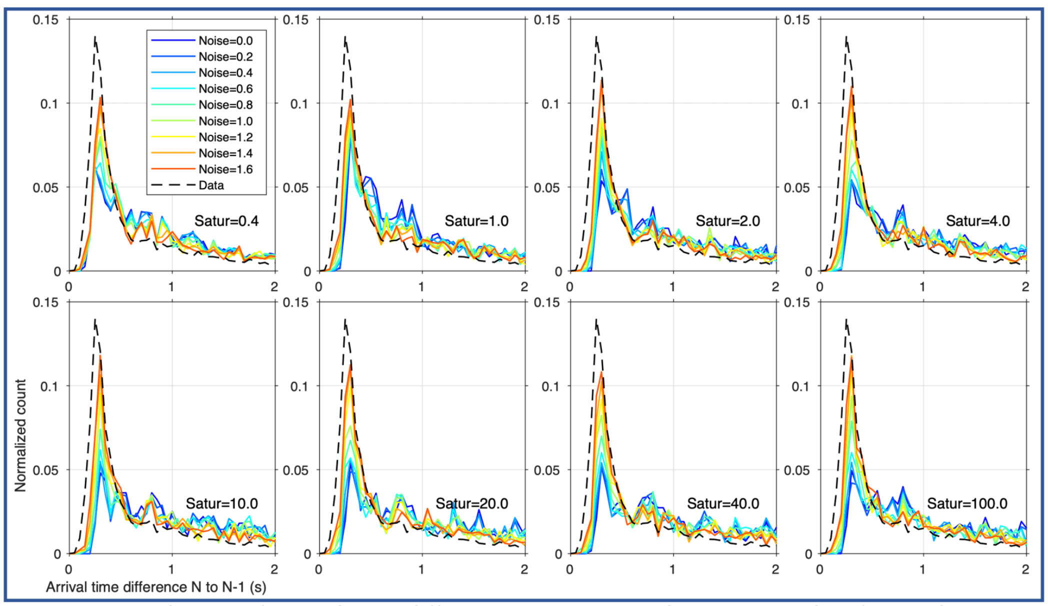

Fig. 13 Distribution of arrival time difference N to N-1, similar to Fig. 10, but for single-spot synthetics.

CONCLUSION

1. The separation of close-in-time LFE sources deconvolved from tremor in SVI along the propagation direction is about 500 m. If LFEs are close to the upper size limit, successive events are strongly overlapping, which seems more consistent with the stochastic acceleration and deceleration model of LFE generation. If, instead, LFEs are brittle asperities closer to 100 m in size, successive events need not overlap, but one must explain both their long duration and why, with so many sources in close proximity, nearly none are observed to grow larger in both duration and magnitude than is characteristic of LFEs.

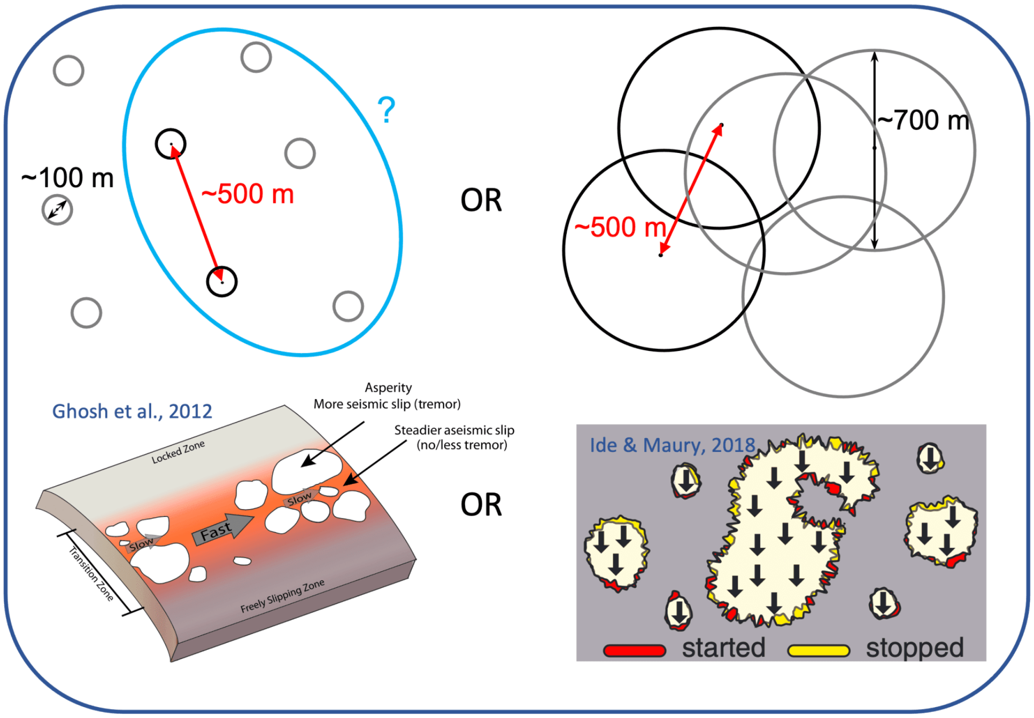

2. SVI Tremor seismograms are saturated in time with LFE arrivals, in the sense that only 30% of the catalog events are separated from their neighbours by more than the characteristic LFE duration (~0.25 s). **Moreover, there is no obvious evidence that tremor loses saturation in time with decreasing amplitude.**

3. To match the waveform CC and separation of sources, in the noise-free case, a 4.2 km x 3 km area is what we think the source region is likely to be. If sources are coming from a single spot, and the scatter we see is due to the noise, then the median amplitude of noise may not exceed roughly 1.3 times that of the signal itself. However, the simulations we present here are two extremes, **the reality may be a combination of source region size and noise level somewhere in between.**

4. If, as expected from the destructive interference inherent in saturated seismograms, ten-times-louder tremor implies 100 times the LFE rate, and given the tremor amplitude range of one order of magnitude, then if quiet tremor is saturated, and if sources are non-overlapping, then **to accommodate all the sources implied during loud tremor in an ellipse of 4.2 km x 3 km, an upper bound on the LFE source dimension is roughly 300 m**.

***5.** Deconvolution of observed and synthetic seismograms seems to suggest a time-varying source saturation. Instead of using a Poissonian distribution for LFE occurrence in time, one might try **a stochastic Brownian-motion source time function**, similar to the seismic moment-rate function defined in (*6*).

AUTHOR INFO

Hi there, my name is Chao Song. I am a PhD candidate in Geosciences at Princeton University. I expect to graduate to in May 2024, keen for a postdoc position! I have a particular interest in understanding the physical nature of LFEs and tremor, and further that of the slow earthquakes using different methods and from various perspectives, to answer why they appear to be so different from regular (fast) earthquakes. I also have a general interest in Seismology and Tectonophysics. I am actively seeking a postdoc postion to continue my research in slow earthquakes. If you found my research interesting, I'd like to talk more about it with you. Shoot an email to me at chaosong@princeton.edu any time should you have any question!

TRANSCRIPT

ABSTRACT

Low Frequency Earthquakes (LFEs) have been viewed as isolated, stick-slip asperities on an otherwise creeping fault, or as the high-frequency limit of stochastic fluctuations of sliding speed on a seismogenic fault. In the former interpretation, the LFE source has frictional properties different from its surroundings, and each represents a co-located acceleration/deceleration. In the stochastic, extended-source-region model of Ide, the accelerations and decelerations that comprise "LFEs" are not necessarily co-located, and most of the underlying seismic moment lies outside the roughly 1-8 Hz band of good signal-to-noise ratio. Here we explore the constraints that LFE locations from an iterative deconvolution of tremor records, using stacked LFE templates as Green's functions, can place on the physical interpretation of tectonic tremor.

Over an amplitude range that spans an order of magnitude, tremor seismograms from southern Vancouver Island appear saturated with LFE arrivals, in the sense that inter-event times are less than the characteristic LFE duration (~0.25 s). Quantitatively, about 46% of consecutive LFEs detected via iterative deconvolution are separated by roughly this duration, independent of tremor amplitude, meaning that quiet tremor is not resolvably less saturated than loud tremor, consistent with Ide's stochastic model.

To estimate plausible source dimensions, we make synthetic saturated seismograms using templates from LFE family 002 of Bostock et al., with no added noise. We find that to match tremor observations from that same region, such as the cross-correlation coefficients between the various stations, and the ~500 m median spacing between nearly contemporaneous LFEs in the low-error direction, the tremor source region active at one time should be not much larger than about 3.5 × 4.9 km. If, as expected from the destructive interference inherent in saturated seismograms, and as in the simplest version of Ide's stochastic model, ten-times-louder tremor implies 100 times the LFE rate, then the above tremor source size places an upper bound on the LFE source dimension of roughly 400 m, a number we hope to refine (reduce) by adding noise to the synthetic seismograms. This size is still large enough for LFEs to be elastodynamic events, given a reduced shear wave speed in the source region.

REFERENCES

1. Ghosh, A., Vidale, J. E., & Creager, K. C. (2012). Tremor asperities in the transition zone control evolution of slow earthquakes. Journal of Geophysical Research: Solid Earth, 117(B10).

2. Ide, S., & Maury, J. (2018). Seismic moment, seismic energy, and source duration of slow earthquakes: Application of Brownian slow earthquake model to three major subduction zones. Geophysical Research Letters, 45(7), 3059-3067.

3. Kikuchi, M., & Kanamori, H. (1982). Inversion of complex body waves. Bulletin of the Seismological Society of America, 72(2), 491-506.

4. Ligorría, J. P., & Ammon, C. J. (1999). Iterative deconvolution and receiver-function estimation. Bulletin of the seismological Society of America, 89(5), 1395-1400.

5. Ohta, K., & Ide, S. (2017). Resolving the detailed spatiotemporal slip evolution of deep tremor in western Japan. Journal of Geophysical Research: Solid Earth, 122(12), 10-009.

6. Ide, S. & Maury, J., 2018. Seismic moment, seismic energy, and source duration of slow earthquakes: Application of Brownian slow earthquake model to three major subduction zones, Geophysical Research Letter, 45(7), 3059–3067.